



Automatic Nuclei Detection in Histopathological Images based on Convolutional Neural Networks

Roaa Safi Abed Alah¹, Gokhan Bilgin^{1,2} ^a and Abdulkadir Albayrak^{1,2} ^b

¹*Dpt. of Computer Engineering, Yildiz Technical University, 34220 Istanbul, Turkey*

²*Signal and Image Processing Laboratory (SIMPLAB), Yildiz Technical University, 34220 Istanbul, Turkey*

Keywords: Nuclei Detection, Histopathological Images, FCM Algorithm, Convolution Neural Networks, Deep Learning.


Abstract: Analysis of cells in histopathological images with conventional manual methods is relatively expensive and time-consuming work for pathologists. Recently, computer aided and facilitated researches for the diagnostic algorithms have obtained a high significance to assist the pathologists to extract cellular structures. In this paper, we are comparing the conventional fuzzy c-means (FCM) clustering method with the proposed automated detection system based on Tiny-Convolutional Neural Network (Tiny-CNN) to detect center of nucleus in histopathological images. Also, in this study, we are tried to find center of nucleus by combined unsupervised method (FCM) with supervised method (Tiny-CNN). Briefly, First step, nuclei centers are detected with FCM algorithm which is applied as a clustering-segmentation method to perform segmentation of nucleus cellular and nucleus non-cellular structure to find the correct center of nuclei. Second step, the deep learning method is used to detect center of nucleus based automated method. Afterward, combined each of these individual methods to evaluate our model for extracting the center of nucleus on two different data set the University of California Santa Barbara's UCSB-58 data set and data set University of Warwick's CRC-100 data set.


1 INTRODUCTION

Histopathological image analysis has various challenges, especially in nucleus detection. The developments in techniques that have been occurred in this area can be a valuable assistance to the accurate diagnosis pathologically. However, it is still harder to reach more details without solving the main complicated issues in cellular structures especially the cluttering problem in tissue (Moita et al., 2018). The cellular structure analysis is significant in pathological diagnoses of breast cancer which depends on cell analysis separately (Albayrak and Bilgin, 2016).

Traditionally, seed detection is a classical problem of computer vision for the conventional of histopathological images. New researches have implemented conventional methods various ways of deep learning scenarios, and scenarios connecting both methods. A graph-cut methods took the place by multi-scale filtering (LoG), adaptive scale selection, and a second graph-cut operation (Al-Kofahi et al., 2010). Nucleus detection in recent year, using of pre-processing

morphological methods assists to smooth and remove non-nuclei objects from input images. Generalized LoG filters and mean-shift clustering were employed to detect nuclei seeds centers and false nucleus were removed by adaptive thresholding (Xu et al., 2017). Apply of generalized LoG (gLoG) filters to develop correctly guess of nucleus shape detector performance and used watershed segmentation technique to separate nucleus and count cells (Kong et al., 2013). The domain of FCM for detecting nucleus positions of feature similarity index measure FSIM is used as seeds for segmentation, this method is started with FCM clustering and then using FSIM based template matching approach for nucleus detection. FCM in probabilistic model and a derivation of an algorithm for FCM clustering which is supplied expanded ability through the conventional FCM (John et al., 2016). This study which is known as Bayesian Fuzzy Clustering that has extended each of variable number of clusters and a particle filters dedicated technique to evaluate the model parameter included the number of clusters (Glenn et al., 2015). Detection of nuclei in an automated methods of histopathological images is represented as a good method. Especially, in recent year with development in machine learning methods

^a  <https://orcid.org/0000-0002-5532-477X>

^b  <https://orcid.org/0000-0002-0738-871X>

which is displayed an effective way of detecting a cell in an image by predicting for each pixel location. One of these methods has discovered the location of each pixel that is the monotonous function of the distance to evaluate the closest cell to the center. Then the cell center can be specified by extracting local extremism of the predicted values (Kainz et al., 2015). While Stacked Sparse Autoencoder (SSAE) method is presented to solve the complexity of automated nuclei detection. A deep learning method is applied to detect an effective nuclei on high-resolution histopathological images of breast cancer which is learning high-level features in just one-pixel intensity to recognize distinctive features of nucleus with a good results (Xu et al., 2016). Authors have proposed a method based on convolution neural networks for detection of the nuclei of cells in images with overlapped cells. CNN is trained from all patches extracted from the training images, which the center of pixel in training patch are classified to three classes, background, cytoplasm, and nucleus. To make network learn how to guess right classify of each central pixel of the patches (Braz and Lotufo, 2017). This method that applied the colour deconvolution to reconstruct all of the applied stains. In addition, the structure of a large feature set and modification AdaBoost to create two detectors that focused on various features in the appearance of nuclei and modified of AdaBoost, is able to calculate the cost of each feature during the selection of nuclei. The output of each detector is incorporated by the optimal active contour algorithm to smooth the border of detected nuclei (Vink et al., 2013).

A convolution neural network with the LoG filter is applied to histopathological images for performing nuclei detection by sliding window to whole image. Application of this method in histopathological images performs promising results in nuclear detection (Khoshdeli et al., 2017). The CNN based deep learning algorithm with superpixel analysis has shown improved segmentation performance for nuclei segmentation while comparing with the state-of-the-art methods. This method, over-segmenting the original image by generating superpixels which allow the CNN to learn the localized features better in the training stage. In another study, Spatially Constrained Convolutional Neural Network (SC-CNN) which forced spatial constraint at the prediction of the likelihood of a pixel by assigning higher probability values to the pixels located in the vicinity of the nuclei centers is implemented for nucleus detection. In that study the classification of nuclei is presented a Neighboring Ensemble Predictor method (NEP) combined with convolution neural network. That provides a good availability in the results of joint detection and

classification of the proposed SC-CNN and NEP (Sornapudi et al., 2018),(Sirinukunwattana et al., 2016). Automatic cell segmentation in histopathological images via two-staged superpixel-based algorithms has been studied in (Albayrak and Bilgin, 2018).

The goal in our study is to detect the center of nuclei on histopathological images, using FCM clustering which is extracted the foreground from background cellular structure of histopathological images. FCM obtained a high accuracy in clustering in order to increase the ability of detecting center of nuclei in conventional method with automated center detection by using convolutional neural networks.

The organization of the paper is as follows: In section 2 we describe the methodology of the study. Section 3 describes the materials used, Nucleus detection and technical details. Section 4 refers to results and discussion, and Section 5 concludes the paper.

2 MATERIAL AND METHODS

In medical image technology had become possible to obtain more meaningful information by applying pre-processing of histopathological images. In recent years, the development which happens in deep learning architectures, had increased quality of data analysis to obtain more information of related image.

2.1 Fuzzy C-means Algorithm

Clustering method is a method of locating a set of objects into group. In this instance, the clustering algorithms can be classified into two classes classes: hard clustering and soft (fuzzy) clustering. One is hard clustering; second one is soft clustering. In this paper, a soft clustering method, fuzzy c-means, is applied to obtain cellular structures in histopathological images. Soft clustering FCM in many cases more resilient than other hard clustering method. In soft clustering, data elements belong to more than one cluster, and associated with each element is set of membership levels as mentioned in (Suganya and Shanthi, 2012). In the nature work of FCM algorithm is depend on assigning membership for each class which is based on degrees among zero and one, to indicate their partial membership. The clustering centers calculated in FCM is shown in Eq. 1:

$$C_j = \frac{\sum_{i=1}^n u_{ij}^m x_i}{\sum_{i=1}^n u_{ij}^m} \quad (1)$$

where, j stands for each cluster center, x_i is the objects in j and u_{ij} is the degree of membership of x_i , the value u_{ij} is the degree of membership of x_i in cluster j and, m is representing any real number bigger than 1.

The membership matrix of u_{ij} is calculated by using x_i and c_j as follows:

$$u_{ij} = \frac{1}{\sum_{k=1}^c \left(\frac{d_{ij}}{d_{kj}}\right)^{2/m-1}} \quad (2)$$

The FCM algorithm works by choosing the membership to each of data point identical to each cluster center depending on the distance between the cluster center and the data point the data which is closer to the cluster center (Hafiane et al., 2008).

2.2 Convolutional Neural Networks (CNN)

Convolutional neural network is a deep learning based algorithm proposed by Lecun et al. to classify handwriting digit images (LeCun et al., 2010). CNN is consisted of three main types of layers: convolutional layer, pooling layer and output layer. Convolution layers, pooling layer, and an output layer. Network layers are compatible in a feed-forward, back-propagation neural networks construction: each convolution layer is followed by a pooling layer, and the last convolution layer is followed by the output layer. The convolution and pooling layers are represented as two-dimensions layers, while the output layer is considered as a 1-D layer. In convolutional neural network, each 2 dimension layer has several levels. In one level it can observe neurons that are arranged in a 2-D array. Also, with respective of the output layer we can obtain a feature map.

In a convolutional layer, each level is linked to one or more feature maps of the next layer. This connection is adjust together with a convolution mask, that is a two-dimensional matrix of adaptable entries weights term. All levels computes the convolution among its two-dimensional inputs and its convolution masks. The convolution outputs are collected and added weight and bias. Then, an activation function is utilized in the result to gain the output which is a 2-D matrix recognized as a feature map. A convolution layer output generate one or more feature maps. All feature map is connected to exactly one level in the output of the convolution feature map as shown in Eq. 3:

$$k_n^l = f_l\left(\sum_{i \in v_n^l} k_i^{(l-1)} \otimes w_{i,n}^l + b_n^l\right) \quad (3)$$

where l stands for the number of layers in the layers numbers in the neurons of network f_l defines as activation function, k_n^l is a feature map output with size $H^{(l-1)} \times W^{(l-1)}$ pixels, size of mask convolution mask in this equation $H^{(l-1)-r_l+1} \times W^{(l-1)-c_l+1}$, with \otimes as 2D convolution operator v_n^l represents list of levels in layers 1-1. Pooling layer is applied to decrease the size of the feature map for further analysis in the next layers. As an example, the sum of four pixels is calculated and multiplied with weight before it is added to bias term. Then the result is sent to the activation function to obtains an output for the 2×2 block. At the end, each pooling level minimize its input size into half, along each dimension. A feature map in this layer is connected to one or more level, then it must be connected with next convolution layer feature map for this layer obtained by Eq. 4:

$$k_n^l = f_l(z_n^{(l-1)} \times w_n^l + b_n^l) \quad (4)$$

where, the feature map n is divided into blocks each of them consist of 4 pixels (2×2) in layer (1-1), where $z_n^{(l-1)}$ is a matrix of that result concluded from the four pixels in $(l-1)$. In the last convolution layer, each level in this layer connected to one of feature map and convolution masks are used that have the exact same size as its input feature maps as proposed in (Hatipoglu and Bilgin, 2017; Phung and Bouzerdoum, 2009). In this study, the center of nuclei detection is proposed in Tiny-CNN and FCM with combined Tiny-CNN, that we obtained a successful result of automated methods with two histopathological data sets of UCSB-58 and CRC-100.

3 EXPERIMENTAL STUDIES

3.1 Histopathological Image Data Sets

The first experimental data set (UCSB-58) is obtained from David Rimm Laboratory in Department of Pathology at Yale University of California, Santa Barbara. The data set is selected from a part of UCSB biosegmentation benchmark and includes 58 set of histopathological images 200×200 size of pixels consist of 32 benign and 26 malignant tissue images (Gelasca et al., 2009). The size of pixel in this images is 896×768 . Additionally, each of this UCSB-58 data set images is corrupted labeled by pathologists to become 200×200 pixels images with ground truth as shown in Fig. 1.

The second data set (CRC-100) is obtained from Department of Computer Science at University of Warwick (Sirinukunwattana et al., 2016). This study

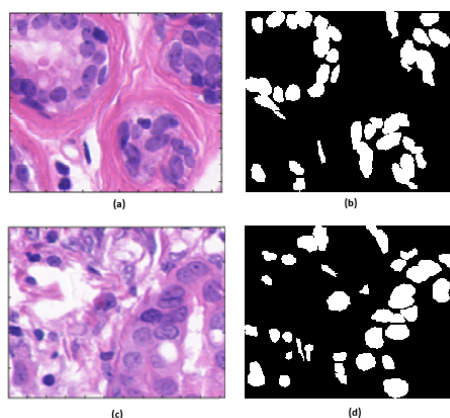


Figure 1: A benign image sample from UCSB-58 histopathological image data set (a) and its ground-truth (b); a malignant image sample (c) and its ground-truth (d).

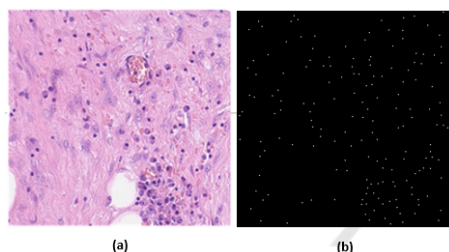


Figure 2: A CRC-100 histopathological image data set sample (a) and its ground-truth (b).

involves all the 10 *E&H* stained histopathological slide images in size of 500×500 at a resolution of $0.55\mu\text{m}/\text{pixel}$ ($20 \times \text{optical}$ magnification). For detection purposes 29,756 nuclei are marked at the center as shown in Fig. 2 and out of 22,444 nuclei centers have an associated class label for classification purpose.

In this paper, we examine FCM clustering result with the results of tiny convolutional neural networks on histopathological images. The concept of this study is consisted of two stages: First, using the clustering method to extract the object from the histopathological images and detecting the center of the object, Second, the detection center of nucleus location that is tried to obtain by Tiny-CNN processing. Third, combined FCM results with Tiny-CNN results.

3.2 Nucleus Detection by using Fuzzy C-Means Clustering Method in Histopathological Images

In this paper, FCM segmentation algorithm is used to detect to detect the center of nucleus of histopathological images. The FCM method is used with two approaches, the first approach is to detect the center of

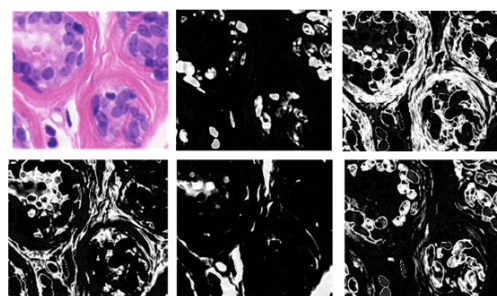


Figure 3: Regional outputs of five different clusters obtained by FCM algorithm.

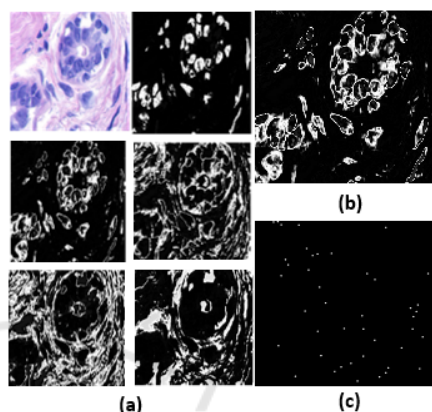


Figure 4: a) Five different cluster regions of FCM algorithm b) obtained nuclei cluster of FCM approach and c) final output nuclei centers image.

nucleus, and the second approach is to segmentation of the nuclei in histopathological images, with mask image for extracting a right nucleus of histopathological images. The FCM semiautomatic approach which means, that we select the closest cluster manually, 5 clusters are selected, since the clusters repeat themselves after five number of clusters as shown in Fig. 3. Then the standard deviation of these clusters are calculated, the maximum standard deviation of these clusters are selected. Afterwards, the closest cluster for the ground-truth accompanied with the data set is selected manually, as shown in Fig. 5c. After finding the closest cluster we apply a morphological operation on the FCM cluster result as shown in Fig. 5d. The FCM automatic mean not chosen manually as shown in Fig. 4b to detect the center of cells as annotated in Fig. 4c, we have experimented this ways which is summarized, finding the maximum Standard deviation of five clusters which are sorted to find the maximum cluster from the candidate clusters to use it for detecting the center of nucleus in histopathological images.

The segmentation steps consist two stages: Firstly, the otsu based thresholding method is applied to each image for extracting the regions of cellular

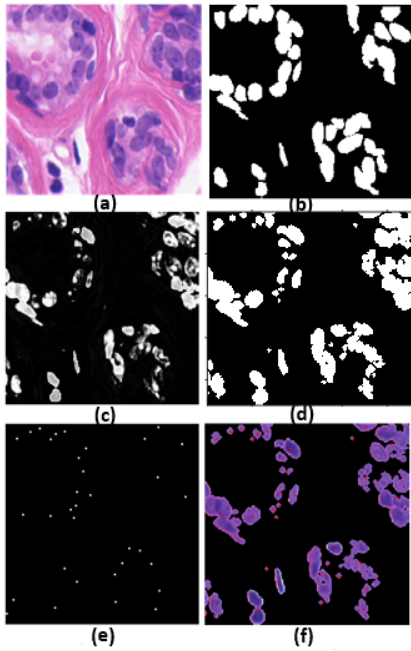


Figure 5: a) An original image from UCSB-58 data set, b) its ground-truth, c) FCM result after choosing closest cluster manually, d) FCM result after morphological operation, e) FCM nuclei center detection and f) masked image of nucleus with center detection.

structures. Then a dilation operation is applied to the result of Otsu's method. After that the binary image obtained from the otsu's method is multiplied to the original image to eliminate the possibly non cellular structures. Binary dilation of A by B , indicated to $A \otimes B$ which is defined as:

$$A \otimes B = \bigcup_z (\widehat{B})_z \cap A \neq \emptyset \quad (5)$$

In this equation, $(\widehat{B})_z$ represents a reflection of the structuring element B . In other words, it is the set of pixel locations z , the reflection structuring element overlaps with foreground pixels in A when translated to z .

3.3 Nuclei Detection by using Tiny- Convolutional Neural Networks

In our model the tiny convolutional neural networks consist of two parts, first part, work as typical CNN building blocks, forward pass learning consist of two layers linear filtering and max pooling, with two terms weight (W) is a $Q \times Q$ filter as shown in Fig. 7b, and the scalar bias (B), with understanding back-propagation, Also, the second layer is connected with the CNN loss layer that contains the derivatives of

the loss (DZDY) of CNN output with respect to positive detection and negative detection in histopathological images. Here, the loss function can be represented as shown below: Where DZDY (Vedaldi and Lenc, 2015) is the derivative of error or loss function, Pos is a positive blobs in histopathological images. Whereas, Neg is a negative blobs or background structure as shown in Eq. 6, and Fig. 7a, Fig. 7b. Convolution neural networks associated with ground truth information which there coordination give as the information of nuclei and background to learn CNN the positive and negative location of nuclei detection as shown in Fig. 6c. Where as, the second part looks at learning two basic CNNs. The first one is a simple non-linear filter capturing particular image structures, while the second one is a network that testing an images (using a variety of different colors).

$$Lossfunction = \frac{Pos}{\sum Pos} - \frac{Neg}{\sum Neg} \quad (6)$$

The first approach in this paper, which is obtaining two data set inputs are used to train Tiny-CNNs with different architectures, and gave the best results accuracy of weight rate or bias from a new value, where the weights are initialized randomly for using $(27 \times 27 \times 3)$ weight initialization. Also, the data set which is used in this study, consist two types of histopathological images which are UCSB-58 data set and CRC-100 data set. We used of training in convolutional neural network, to estimate the centers of nuclei from the best model selection as shown in Fig. 7d. In the UCSB-58 data set histopathological images the network is trained with 58 images in data set. Whereas, in the second data set CRC-100 network trained for 100 images in data set. All the predictions of this algorithm have achieved a good result to detect the center of nucleus location Fig. 7g. Our study proposes to find nuclei centers with Tiny-CNN. To accomplish this task, we used the combined operation(combined the detection center of nuclei of FCM semi automatic method with Tiny-CNN center detection). Our proposed study is detected the center of nucleus by using conventional FCM clustering method, on the original of histopathological image. This image is used to compere with Tiny-CNN prediction the center of nucleus. Also, apply a semi-automatic FCM algorithm for extracted the perfect nucleus of histopathological images, and find the center of nuclei, to compere it also with Tiny-CNN result, Then, we experment the result of combined this approach with Tiny-CNN based automated method as shown in Fig. 8. This scenario is applied on two data set CRC-100 data set is accompanied with coordination (x,y) ground truth information and UCSB-58 data set with

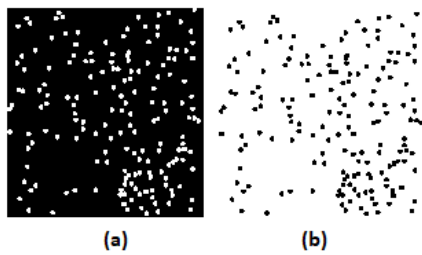


Figure 6: a) Detected positive nuclei centers for a sample image in CRC-100 data set obtained by Tiny-CNN and b) its negative image.

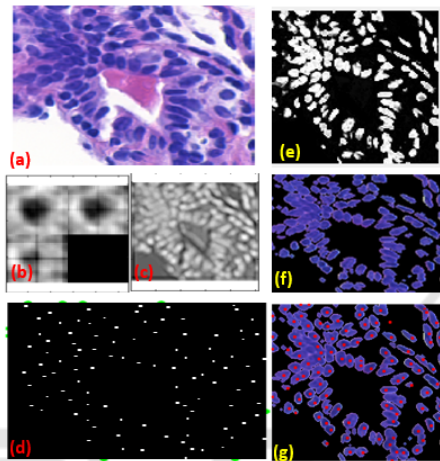


Figure 7: a) Original image from UCSB-58 data set, b) the result of filtering, c) Tiny-CNN output image detect of nuclei, d) final output result of Tiny-CNN detect center of nuclei, e) FCM semiautomatic result, f) generated mask from the FCM semiautomatic result combined with original image g) used mask image with Tiny-CNN output the center of the nuclei detection.

our contribution ground truth which is choose the coordinates of (x,y) manually with the same manners of CRC-100 data set ground truth.

4 RESULT AND DISCUSSION

In the detection of nuclei in histopathological images three approaches (Tiny-CNN, FCM, FCM-semi-automatic) are evaluated and compared detection center of nuclei in two different data set UCSB 58-set and CRC 100-set. Our contributions include a dot operator, by clicking on the center of a nuclei manually to produce ground truth information, for the first data set UCSB-58 data set to obtain the same manner of ground-truth information in the CRC-100 data set. This ground truth information can also be seen in this study to detect the center of nuclei in histopathological images. The first approach uses detecting center of

cell by Tiny-CNN, second approach using FCM and FCM semi-automatic algorithm to detect the center of nuclei, then, that we compared these two approaches to find the best results for center of nucleus detection. Afterwards, we combined center of nuclei result of the Tiny-CNN and FCM semi-automatic approaches to evaluate our model in detect center of nuclei. The basic experimental results unit in this study, has used the boundary of cell size to detected the correct nuclei in related image. In the first data set UCSB-58 data set we stand a region information around 20 pixel as circular regions. Whereas, in the second data set CRC-100 data set, we stand the circular regions within 10 pixels of each cell in the histopathological image. A detection can be evaluated of cell center is identified to be a true positive (TP) when it is matched within the ground-truth information, otherwise, it is represent as a false positive (FP). Every true positive is incorporated with the nearest ground-truth cell center. The ground-truth cell centers that are not marched by any detected results are represented as false negatives (FN). The accuracy of nucleus detection is calculated on a per nucleus basis on recording the true positive (TP) (correctly identified nucleus successfully detected), false negative (FN) (incorrectly rejected nucleus), and false positive (FP) (identified non nucleus objects found). In Fig. 9 the ground-truth results with Tiny-CNN results. In this study the automated method, contributors achieve results as shown in Table 1. Focusing on the F-M measure we have also defined True Positive Rate (TPR) and Positive Prediction Value (PPV). Based on the above definitions, we observe the strongest performance reach to (FM between 0.769 and 0.979) as shown in Table 1. The sensitivity or true positive rate (TPR) is estimated by formula as in Eq. 7:

$$TPR = \frac{TP}{TP + FN} \quad (7)$$

F1-score in Eq. 9 is represented as a metric of overlap between the nuclei predicted and ground-truth information. The F1-score is associated with true positive rate and precision prediction value in Eq. 8 .

$$PPV = \frac{TP}{TP + FP} \quad (8)$$

$$F1 - score = 2 \times \frac{TPR \times PPV}{TPR + PPV} \quad (9)$$

$$DSC = \frac{2TP}{2TP + FP + FN} \quad (10)$$

Dice Similarity Coefficient (DSC) in Eq(10), is used as a statistical validation measurement for evaluating the performance of both the predictability of

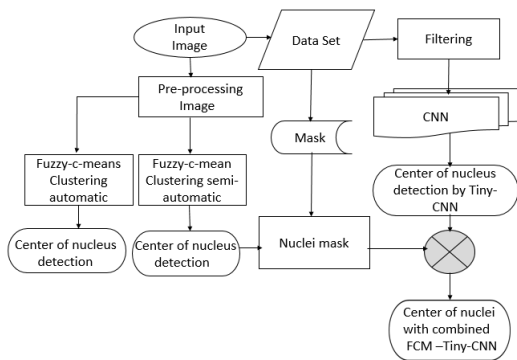


Figure 8: Proposed methodology, comparing FCM center detection with Tiny-CNN center detection, combined FCM and Tiny-CNN to detect center of nuclei.

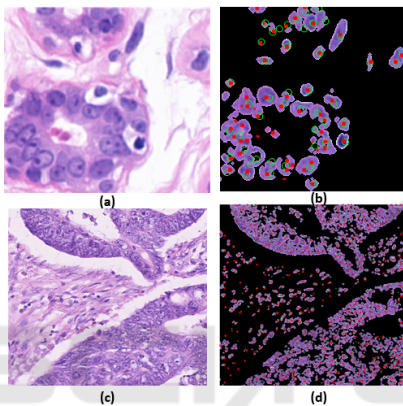


Figure 9: a) An example image of UCSB-58 data set and, b) red points represent outputs of nucleus center detection by Tiny-CNN; green circles refer to ground truth information. c) An example image of CRC-100 data set and, d) output of detected nucleus centers Tiny-CNN and ground-truth.

manual segmentation and the overlap accuracy of automated segmentation of histopathological images.

All information about the experimental results about detection of nuclei in histopathological images in this study, are shown in Table 1. Each different method in this study gives different performance. In this paper, the proposed methods have obtained a true positive rate (TPR) of nucleus center detection that has reached between (0.863 - 0.964) at UCSB-58 data set consisting of 58 images. In addition, in this data set the (F-M or F1-score) has reached to 0.979 in Tiny-CNN and 0.934 in the combined FCM and Tiny-CNN, and other FCM approaches reached between (0.89 - 0.933), whereas, in CRC data set the true positive rate (TPR) has obtained results between (0.547 - 0.621) and (F-M) has reached between (0.528 - 0.769). In this instance, the evaluating of boundary in this study, has a direct effect on the true positive rate (TPR) as shown in Table 1.

5 CONCLUSIONS

In this study, we evaluated and compared fuzzy C-means (FCM) clustering algorithm with tiny convolutional neural network to detect center of nuclei in histopathological images. To further explore nuclei in data set images we combined and experimented two approaches (Tiny-CNN and FCM semi-automatic) as shown in Fig. 8. High results performance in (F-M) reach to (between 0.899 - 0.979) are observed in the first data University of California Santa Barbara's UCSB-58 set. However, we also observed in the second, data set University of Warwick's CRC-100 set, the highest results performance in (F-M) between (0.741 - 0.769). In our models, the basis for the qualitative form similarity between model prediction and ground truth information to detect nuclei in histopathological images. The correct nuclei is detected, according to ground-truth information as shown in Fig. 9, it has shown that the prediction of Tiny-CNN method with ground-truth information on the UCSB-58 and CRC-100 data sets.

The future work of this study, we will consider comparing performance of Tiny-CNN with other CNN established method to detect nuclei in histopathological images.

REFERENCES

- Al-Kofahi, Y., Lassoued, W., Lee, W., and Roysam, B. (2010). Improved automatic detection and segmentation of cell nuclei in histopathology images. *IEEE Trans. on Biomedical Engineering*, 57(4):841–852.
- Albayrak, A. and Bilgin, G. (2016). Mitosis detection using convolutional neural network based features. In *IEEE 17th Int. Symposium on Computational Intelligence and Informatics, CINTI'16*, pages 335–340. IEEE.
- Albayrak, A. and Bilgin, G. (2018). Automatic cell segmentation in histopathological images via two-staged superpixel-based algorithms. *Medical & Biological Engineering & Computing*, pages 1–13.
- Braz, E. F. and Lotufo, R. (2017). Nuclei detection using deep learning. *Simpósio Brasileiro de e Processamento de Sinais*, pages 1059–1063.
- Gelasca, E. D., Obara, B., Fedorov, D., Kvilekval, K., and Manjunath, B. (2009). A bio-segmentation benchmark for evaluation of bioimage analysis methods. *BMC Bioinformatics*, 10(1):368.
- Glenn, T. C., Zare, A., and Gader, P. D. (2015). Bayesian fuzzy clustering. *IEEE Transactions on Fuzzy Systems*, 23(5):1545–1561.
- Hafiane, A., Bunyak, F., and Palaniappan, K. (2008). Fuzzy clustering and active contours for histopathology image segmentation and nuclei detection. In *Int. Conf. on Advanced Concepts for Intelligent Vision Systems*, pages 903–914. Springer.

Table 1: Nuclei detection results with UCSB-58 and CRC-100 histopathological image data sets by using Tiny-CNN and FCM semiautomatic, automatic method, and, combined FCM semiautomatic with Tiny-CNN.

Data Set	TPR	PPV	F-M	DSC
UCSB-58 set with Tiny-CNN	0.964	0.996	0.979	0.979
UCSB-58 set with FCM semiautomatic	0.881	0.994	0.933	0.933
UCSB-58 set with FCM automatic	0.828	0.994	0.899	0.899
CRC-100 set with Tiny-CNN	0.621	0.989	0.769	0.769
CRC-100 set with FCM semiautomatic	0.466	0.994	0.617	0.617
CRC-100 set with FCM automatic	0.451	0.994	0.528	0.528
UCSB-58 set with combined FCM and Tiny-CNN	0.863	0.994	0.934	0.934
CRC-100 set with combined FCM and Tiny-CNN	0.547	0.967	0.741	0.741

Hatipoglu, N. and Bilgin, G. (2017). Cell segmentation in histopathological images with deep learning algorithms by utilizing spatial relationships. *Medical & Biological Engineering & Computing*, 55(10):1829–1848.

John, J., Nair, M. S., Kumar, P. A., and Wilscy, M. (2016). A novel approach for detection and delineation of cell nuclei using feature similarity index measure. *Biocybernetics and Biomedical Engineering*, 36(1):76–88.

Kainz, P., Urschler, M., Schultze, S., Wohlhart, P., and Lepetit, V. (2015). You should use regression to detect cells. In *International Conference on Medical Image Computing and Computer-Assisted Intervention*, pages 276–283. Springer.

Khoshdeli, M., Cong, R., and Parvin, B. (2017). Detection of nuclei in H&E stained sections using convolutional neural networks. In *IEEE EMBS Int. Conf. on Biomedical & Health Informatics, BHI'17*, pages 105–108.

Kong, H., Akakin, H. C., and Sarma, S. E. (2013). A generalized laplacian of gaussian filter for blob detection and its applications. *IEEE Transactions on Cybernetics*, 43(6):1719–1733.

LeCun, Y., Kavukcuoglu, K., Farabet, C., et al. (2010). Convolutional networks and applications in vision. In *ISCVS*, volume 2010, pages 253–256.

Moita, A. S., Jacinto, F., and Moreira, A. L. N. (2018). Design, test and fabrication of a droplet based microfluidic device for clinical diagnostics. In *Proceedings of the 11th Int. Joint Conference on Biomedical Engineering Systems and Technologies-Volume 1: BIODEVICES, BIOSTEC'18*, pages 88–95. INSTICC, SciTePress.

Phung, S. L. and Bouzerdoum, A. (2009). Matlab library for convolutional neural networks. *University of Wollongong, Tech. Rep.*, URL: <http://www.elec.uow.edu.au/staff/sphung>.

Sirinukunwattana, K., Raza, S. E. A., Tsang, Y.-W., Snead, D. R., Cree, I. A., and Rajpoot, N. M. (2016). Locality sensitive deep learning for detection and classification of nuclei in routine colon cancer histology images. *IEEE Trans. on Medical Imaging*, 35(5):1196–1206.

Sornapudi, S., Stanley, R. J., Stoecker, W. V., Almubarak, H., Long, R., Antani, S., Thoma, G., Zuna, R., and Frazier, S. R. (2018). Deep learning nuclei detection in digitized histology images by superpixels. *Journal of Pathology Informatics*, 9.

Suganya, R. and Shanthi, R. (2012). Fuzzy c-means algorithm-a review. *Int. Journal of Scientific and Research Publications*, 2(11):1.

Vedaldi, A. and Lenc, K. (2015). Matconvnet: Convolutional neural networks for matlab. In *Proceedings of the 23rd ACM International Conference on Multimedia*, pages 689–692.

Vink, J. P., Van Leeuwen, M., Van Deurzen, C., and De Haan, G. (2013). Efficient nucleus detector in histopathology images. *Journal of Microscopy*, 249(2):124–135.

Xu, H., Lu, C., Berendt, R., Jha, N., and Mandal, M. (2017). Automatic nuclei detection based on generalized laplacian of gaussian filters. *IEEE Journal of Biomedical and Health Informatics*, 21(3):826–837.

Xu, J., Xiang, L., Liu, Q., Gilmore, H., Wu, J., Tang, J., and Madabhushi, A. (2016). Stacked sparse autoencoder (SSAE) for nuclei detection on breast cancer histopathology images. *IEEE Transactions on Medical Imaging*, 35(1):119–130.